University of South Carolina College of Engineering and Computing Mechanical Engineering Department

Parametric Study of Pool Boiling on Horizontal Highly Conductive Microporous Coated Surfaces

Chen Li, G. P. Peterson

Parametric Study of Pool Boiling on Horizontal Highly Conductive Microporous Coated Surfaces

Chen Li
Assistant Professor
Mem. ASME
e-mail: lichen.cu@colorado.edu

G. P. Peterson
Professor and Chancellor
Fellow ASME
e-mail: bud.peterson@colorado.edu

Department of Mechanical Engineering,
University of Colorado at Boulder,
Boulder, CO 80309-0427

To better understand the mechanisms that govern the behavior of pool boiling on horizontal highly conductive microporous coated surfaces, a series of experimental investigations were designed to systematically examine the effects of the geometric dimensions (i.e., coating thickness, volumetric porosity, and pore size, as well as the surface conditions of the porous coatings) on the pool-boiling performance and characteristics. The study was conducted using saturated distilled water at atmospheric pressure (101 kPa) *and porous surfaces fabricated from sintered isotropic copper wire screens. For nucleate boiling on the microporous coated surfaces, two vapor ventilation modes were observed to exist: (i) upward and (ii) mainly from sideways leakage to the unsealed sides and partially from the center of porous surfaces. The ratio of the heater size to the coating thickness, the friction factor of the two-phase flow to single-phase flow inside the porous coatings, as well as the input heat flux all govern the vapor ventilation mode that occurs. In this investigation, the ratio of heater size to coating thickness varies from 3.5 to 38 in order to identify the effect of heater size on the boiling characteristics. The experimental results indicate that the boiling performance and characteristics are also strongly dependent on the volumetric porosity and mesh size, as well as the surface conditions when the heater size is given. Descriptions and discussion of the typical boiling characteristics; the progressive boiling process, from pool nucleate boiling to film boiling; and the boiling performance curves on conductive microporous coated surfaces are all systematically presented.* [DOI: 10.1115/1.2759969]

Keywords: parametric study, microporous surface, boiling characteristics, boiling performance

1 Introduction

The practice of using rough or microstructured surfaces to enhance the boiling performance and increase the CHF has been of considerable interest since it was first observed and reported by Jakob in 1931 [1]. Since that time, considerable effort has been devoted to the development of artificial surfaces and structures in order to improve nucleate boiling as well as increase the critical heat flux (CHF) for long-term operation and applications. Until 1954, however, enhanced surfaces were thought to be unusable in industrial applications, due to the decay of the enhancement caused by the little-understood "aging effect." This situation changed dramatically with the development of several patents [2–4] that were successfully employed in industry in the mid-1960s. The critical development was the work of Milton [2–4], who achieved high nucleate boiling performance through the sintering of porous coatings on tube surfaces.

Generally speaking, there are three types of enhanced or microstructured surfaces employed in nucleate boiling applications: "pore-and-tunnel" surfaces or reentrant cavities, finned surfaces, and porous media coated surfaces. The latter of these, porous coated surfaces, has been one of the most attractive techniques for enhancing the boiling heat transfer coefficient as well as the CHF for many years. Although the information available in the literature is quite extensive, there is still considerable confusion about the impact of these coatings on the heat transfer and boiling enhancement. As a result, the information presented here is restricted to porous coated surfaces and is intended to clarify the fundamental phenomena that affect the behavior and performance of these surfaces.

In addition to the specific thermophysical properties of the material, porous coated surfaces are most frequently categorized based on their thickness and structure. Experimental and numerical studies [5–18] have consistently demonstrated that nucleate boiling performance can be significantly enhanced, and boiling incipience superheat dramatically reduced, through the use of porous coatings. Investigations have revealed the physical processes and specific characteristics of boiling in porous media coated surfaces that are important, such as the location of the evaporation and nucleate boiling sites, the behavior of the liquid and vapor phases, the existence of a vapor film near the heating wall, etc. Moss and Kelly [13] performed neutron radiography of evaporation on a 6.3 mm thick sintered stainless steel wire mesh in which the sides of the porous media were open. A static, time-invariant vapor blanket was observed near the heating wall that appeared to increase in thickness with increasing heat flux. The capillary pressure across the internal liquid vapor interface also increased with increasing heat flux. In this investigation, Moss and Kelly [13] concluded that the phenomenon of vapor escaping from the sides of the wick presented a more realistic interpretation of the results than a model based on evaporation from the surface, and small vapor patches formed inside the wick would not "choke" the liquid supply, but instead, the presence of the porous structure in a boiling fluid would effectively "smooth out the formation" of individual nucleate bubbles and eliminate the sudden transition from nucleate boiling to film boiling.

Cornwell et al. [14] observed the simultaneous and continuous existence of vapor and liquid regions in a 6 mm thick polyurethane foam wick and found that these regions extended through the wick thickness and that the boundaries between the regions

Contributed by the Heat Transfer Division of ASME for publication in the JOURNAL OF HEAT TRANSFER. Manuscript received January 2, 2006; final manuscript received April 10, 2007. Review conducted by Ramendra P. Roy.

were stable. In this investigation, contact between the porous coating and the heated wall was maintained by a rod and perforated plate. The heat flux was observed to increase proportionally with the ratio of the vapor-covered area to the total heating area, A_v/A, and the frictional pressure drop of the vapor flow through the liquid saturated porous wick was found to be much higher than through a dry wick of similar dimensions.

Nakayama et al. [15] believed that boiling in porous media with reentrant grooves, was a highly dynamic process and that three "routes" for the heat transfer from the surface to the ambient liquid existed: convective heat transfer agitated by bubble formation, vaporization of the liquid near the outer surface into the growing bubbles, and vaporization in the tunnel formed by the reentrant grooves. Bergles and Chyu [16] conducted an experimental investigation of boiling on a brazed metal powder, 0.38 mm thick and with volumetric porosities ranging from 50% to 65%. The results of this investigation indicated that nucleate boiling occurs within the porous media from the reentrant cavities, and vaporization occurred within the porous media, forcing the vapor bubbles out. The low boiling incipience superheat was thought to be due to the large internal surface area, with vapor-liquid counterflow occurring during the boiling process. The vapor did not spread evenly over the surface to activate other adjacent sites, due to the internal generation of vapor, instead the random distribution of active sites resulted in what was referred to as "patch boiling."

Polezhaev and Kovalev [17] successfully modeled boiling heat transfer on 1 mm thick porous structures, numerically. In the investigation, Polezhaev and Kovalev [17] assumed that the evaporation occurred inside the porous coatings. Heat was transferred from the heating wall, through the shell of the porous structure, to the meniscus of the liquid, where vaporization occurred. Polezhaev and Kovalev [17] also found that higher effective thermal conductivities could enhance boiling performance and that the maximum evaporation occurs at the bottom of the porous coating at low heat fluxes and then decreases with increasing heat flux, causing the evaporation position to move toward the surface of the porous coating. Malyshenko [10], and Borzenko and Malyshenko [12] conducted a series of experimental and visual studies of boiling on nonconductive porous coatings, and illustrated that the porous coating thickness plays a determining role in the boiling characteristics and that there exists a drying zone, during the boiling process. In this approach, the drying zone corresponds to the thickness and there is a critical drying zone area, which does not change in size until the input heat flux exceeds the CHF. Malyshenko [10] and co-workers observed a vapor film formed near the heating wall for thick porous coatings and found that the thickness of the vapor film was approximately half the thickness of the porous coating. Based on these observations and comparisons to other data, O'Connor et al. [7] hypothesized that the improvement in the heat transfer performance from porous coated surfaces was primarily due to the increase in the number of active nucleation sites.

Based on a review of the literature presented above, and more recent work on boiling in microporous coated surfaces [19,20], it is clear that significant improvements in nucleate boiling heat transfer and reductions in the boiling incipience superheat can be achieved for both conductive and nonconductive materials. In addition, several generalizations regarding pool boiling in porous coatings can be made as follows:

- Nucleate boiling and evaporation, both occur "inside" of the porous media [13,14,16,17].
- Stable internal vapor and liquid counterflow patterns are formed in thick porous coatings during the boiling process [7,9–14,17].
- A thin vapor film is often formed near the heating wall on thick coatings, depending on the magnitude of the heat flux [10–13].
- The frictional pressure drop for vapor flow through a saturated porous media is much higher than through a dry porous media and as a result, the vapor will try to escape from the sides of the porous coating [14].
- Boiling performance increases in porous media may be due to the strong convection caused by the agitation of the vapor bubbles inside of the porous coatings and by the increase in the number of nucleate sites [7,9,15].
- The formation of individual nucleate bubbles is limited in porous media compared to plain surfaces, retarding the formation of film boiling and resulting, instead, in stable "patch boiling." This feature could eliminate the sudden transition from nucleate boiling to film boiling [13,16].
- Boiling performance and characteristics are strongly dependent on the geometric parameters, the thermal properties of the porous media, and the contact conditions between the porous coatings and the heated wall [10–13,15,17].

Although informative, because the conditions for each of these studies varied, these conclusions alone do not provide a sufficiently comprehensive or conclusive description of the boiling in porous coatings and as a result, show only limited guidance as to how to optimize the effect of the various parameters that govern these phenomena. For this reason, a systematic investigation was conducted to examine the effects of the geometric dimensions, i.e., coating thickness, volumetric porosity, and mesh size of microporous surfaces on boiling incipience and nucleation. The ratio of heater size to coating thickness is varied from 3.5 to 38 to investigate the vapor ventilation modes. This parametric study successfully verifies some of the conclusions in previous numerical simulations and has led to further understanding of the boiling characteristics and mechanisms that govern the boiling heat transfer on porous coated surfaces.

2 Experimental Test Facility and Procedure

2.1 Test Articles Structure and Fabrication. In the current investigation, a series of experimental tests were conducted using saturated distilled water at atmospheric pressure, in contact with a horizontal, 8 mm $\times$ 8 mm conductive porous coating. The key geometric parameters of the porous coating, such as the coating thickness, volumetric porosity, and pore size, were varied to determine the effects on the boiling performance and the boiling characteristics. Sintered pure isotropic copper wire screens, similar to those illustrated in Figs. 1(*a*) and 1(*b*) [19], were employed as the conductive microporous media. All sintered copper wire screens are in staggered structure in this experimental study.

The structure of the test articles, which are similar to samples in [19] except for the wing structures, is illustrated in Fig. 2. It consists of three parts: an 8 mm $\times$ 8 mm square, multilayered sintered isotropic copper mesh section; a 0.03 mm thick copper foil; and an 8 mm $\times$ 8 mm square copper heating block with a 7.8 mm threaded cylindrical portion. Three thermocouples, i.e., TC1, TC2, and TC3, are located at the center of the copper bar at 10 mm intervals, from which the steady-state 1D axial heat flux of the copper heating block could be determined by the linear temperature distribution and estimated accurately coupling with the known thermal conductivity of the pure copper. The temperature of the interface between the heating block and wick structure is derived from TC1, which is located at 0.5 mm below the interface. The detailed data reduction process is shown in Sec. 2.3.

An optimal sintering process developed by Li et al. [19] was employed to fabricate the test articles. Test data [19] illustrated that this sintering process could achieve nearly perfect contact conditions. Sintered isotropic copper wire screen was directly sintered to the heating block to avoid the contact thermal resistance at the interface between the porous material and the heating block. The fabrication procedure and sintering process are detailed in [19]. The finished surface is illustrated in Fig. 3.

A total of ten different test articles were evaluated experimentally to determine the effects of the geometric parameters of the

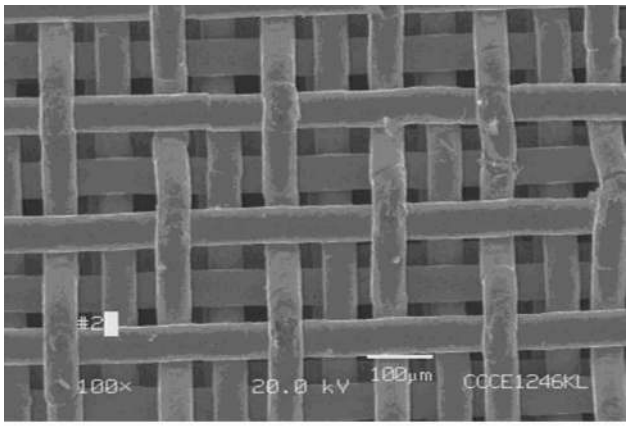

(*a*)

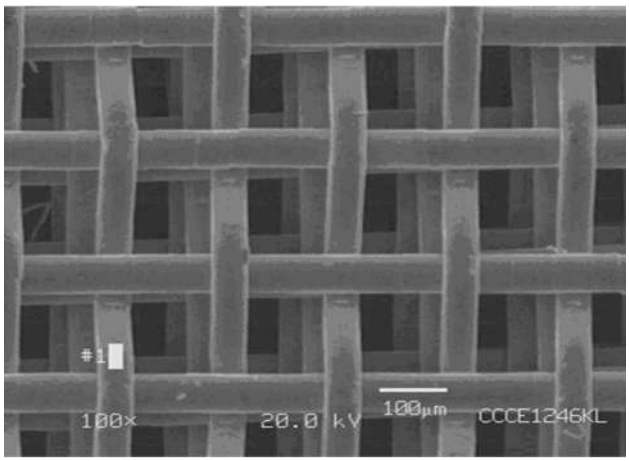

(*b*)

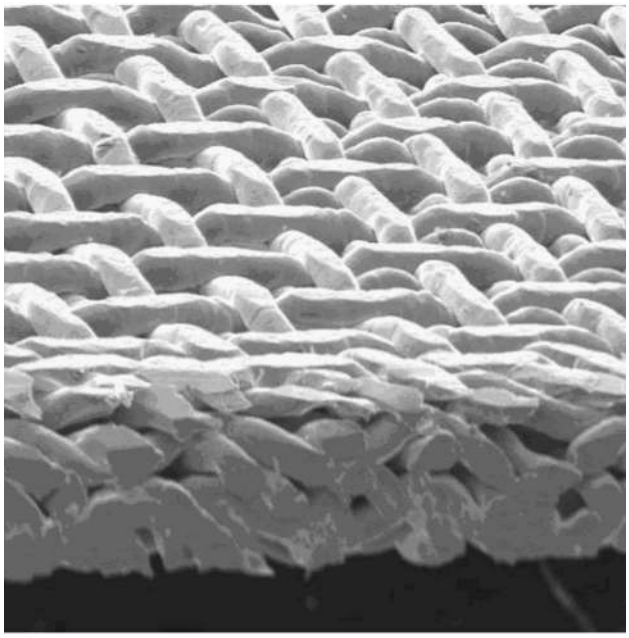

(*c*)

Fig. 1 Scanning Electron Microscope (SEM) images of sintered isotropic copper mesh with 1509 m^{-1} (145 $in.^{-1}$), 56 μm (0.0022 in.) wire diameter, fabricated at a sintering temperature of 1030°C with gas mixture protection (75% N_2 and 25% H_2) for 2 h [19]: (*a*) Top view of staggered sintered isotropic copper mesh [19], (*b*) top view of inline stacked sintered isotropic copper mesh [19], and (*c*) side view of compact sintered isotropic copper mesh [20]

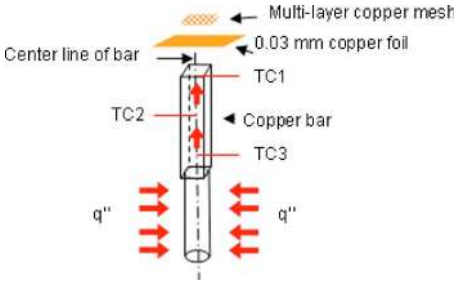

Fig. 2 Schematic of the test article

microporous surfaces on the pool boiling heat transfer performance and characteristics. The specifications of the ten test articles are listed in Table 1, where the variables are highlighted. The test article designations, which describe the specific characteristics for each, are identified. The nomenclature represents the type of boiling, followed by the number of layers and mesh number of the screen, for example, PB145-2 denotes a pool boiling test sample, which is fabricated from two layers of 5709 m^{-1} (145 $in.^{-1}$) copper wire screen.

2.2 Test Facility and Procedure. The experimental test facility is shown in Fig. 4 and has been described in detail in [19]. This test rig consists of an aluminum chamber with two guard heaters, a reservoir for the distilled water supply, a heating system, and a data acquisition system. Compared to the test facility in the film evaporation tests [19], the samples are totally immersed in saturated liquid in the present test.

Nucleate boiling on a plain surface was used to calibrate the experimental test facility [19]. Prior to the recording of any test data, all dissolved gases were removed from the distilled water by boiling for at least 2 h. Three K-type thermocouples (TC4, TC5, and TC6) are used to monitor the water temperature at different positions. The test facility was allowed to reach steady state, defined as the point at which the temperature reading for any thermocouple varied by <0.1°C over a period of 10 min. Then, the steady-state experimental data were averaged over a period of 5 min and recorded at each power level. The power was then incremented and the process repeated, until the CHF had been achieved.

2.3 Data Reduction and Experimental Uncertainties. The processes of data reduction and experimental uncertainties are identical to that described in [19]. The test data were categorized to obtain three key parameters, computed from Eqs. (1)–(3), respectively: the super heat, $T_W - T_{sat}$; the heat flux q'' (including the CHF); and the evaporation/boiling heat transfer coefficient h_{eff}.

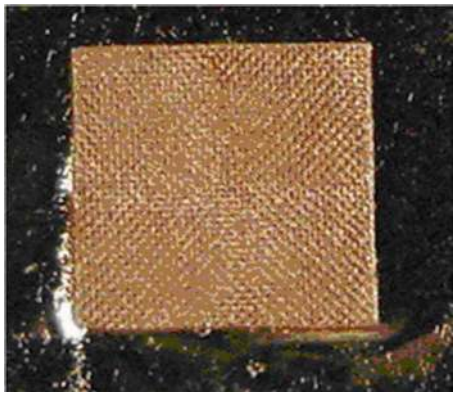

Fig. 3 Image of the completed sintered wire screen surface before the test and after dryout

Table 1 Specifications of the test samples

Grouped by varying	Sample No.	Thickness (mm)	Porosity	Wire diameter (μm)	Pore size (μm)
Thickness	PB145-2	0.21	0.737	56	119.2
	PB145-4	0.37	0.693	56	119.2
	PB145-6	0.57	0.701	56	119.2
	PB145-8	0.74	0.698	56	119.2
	PB145-16	1.38	0.69	56	119.2
	PB145-32	2.30	0.64	56	119.2
Volumetric porosity	PB145-4	0.37	0.693	56	119.2
	PB145-6c	0.36	0.56	56	119.2
	PB145-7c	0.37	0.409	56	119.2
Mesh size (mesh number and wire diameter)	PB145-4	0.37	0.693	56	119.2
	PB100-2	0.36	0.632	114	140
	PB60-1	0.38	0.67	191	232.2

$$T_W - T_{sat} = T_{TC1} - \frac{T_{TC4} + T_{TC5} + T_{TC6}}{3} - \frac{q'' t_{STC1}}{K_{Cu}} \quad (1)$$

$$q'' = \frac{K_{Cu}[(T_{TC3} - T_{TC2}) + (T_{TC2} - T_{TC1})]}{2t_{hole}} \quad (2)$$

$$h_{eff} = \frac{q''}{T_W - T_{sat}} \quad (3)$$

In Eq. (1), $T_{sat}=(T_{TC4}+T_{TC5}+T_{TC6})/3$ and $T_W=T_{TC1}-q''t_{STC1}/K_{Cu}$. Here, the terms T_{TC1}, T_{TC2}, and T_{TC3} represent the temperature for the three K-type thermocouples used to monitor the axial temperature distribution in the copper heater at 10 mm intervals. Thermocouples T_{TC4}, T_{TC5}, and T_{TC6} were used to measure the water temperature in the test chamber. Using this measured temperature, T_{TC1}, and the known thermal conductivity K_{Cu}, the temperature at the bottom of the capillary wick structure T_W was derived; then, using T_{TC1}, T_{TC2}, and T_{TC3}, the heat flux q''dissipated through evaporation/boiling under steady-state conditions could be determined. With these two values, the effective heat transfer coefficient can be estimated from Eq. (3).

The uncertainty of the temperature measurements, the length (or width), and the mass are ±0.5°C, 0.01 mm, and 0.1 mg, respectively. A Monte Carlo error of propagation simulation indicated the following 95% confidence level for the computed results: the heat flux was less than ±5.5 W/cm^2; the heat transfer coefficient was less than ±20%; the superheat ($T_{wall}-T_{sat}$) was less than ±1.3°C, and the volumetric porosity ε was less than ±1.5%.

3 Results and Discussion

The objectives of this investigation are to (i) examine the effects of thickness, volumetric porosity, and mesh size of the porous coatings on the boiling performance, characteristics, and the CHF, and (ii) identify the heat transfer and liquid/vapor phase regimes. All test results are summarized from Figs. 5–9. The heat transfer and the two-phase behavior regimes are presented in Fig. 10. The discussion begins from the general characteristics of nucleate boiling, and then proceeds to the effects of several key geometric dimensions, such as the coating thickness, the volumetric porosity and the mesh size.

3.1 Characteristics of Nucleate Boiling on Microporous Coated Surfaces

3.1.1 Two-Phase Flow Patterns at High Heat Flux. Previous investigations have demonstrated the existence of vapor film and the vapor-liquid countercurrent flow inside porous coatings during boiling [7,9–14,17]. There is also a vapor-liquid separating flow in

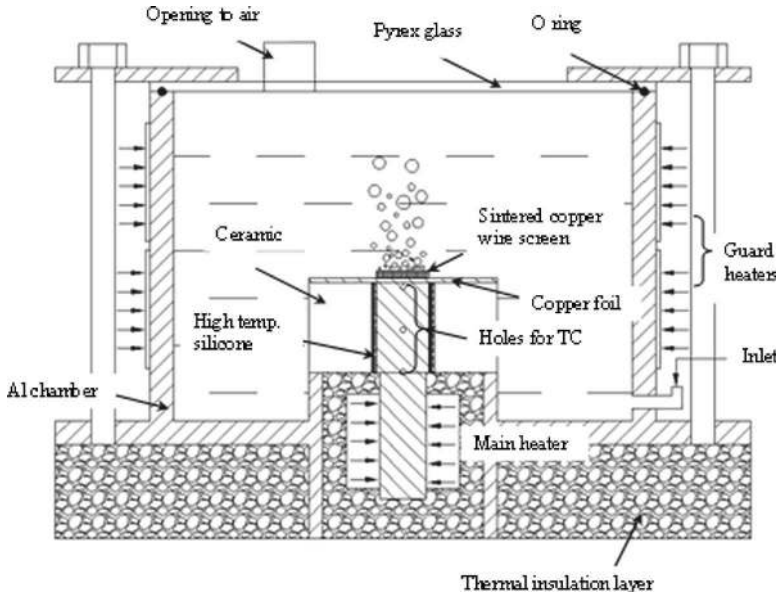

Fig. 4 Schematic of the test facility

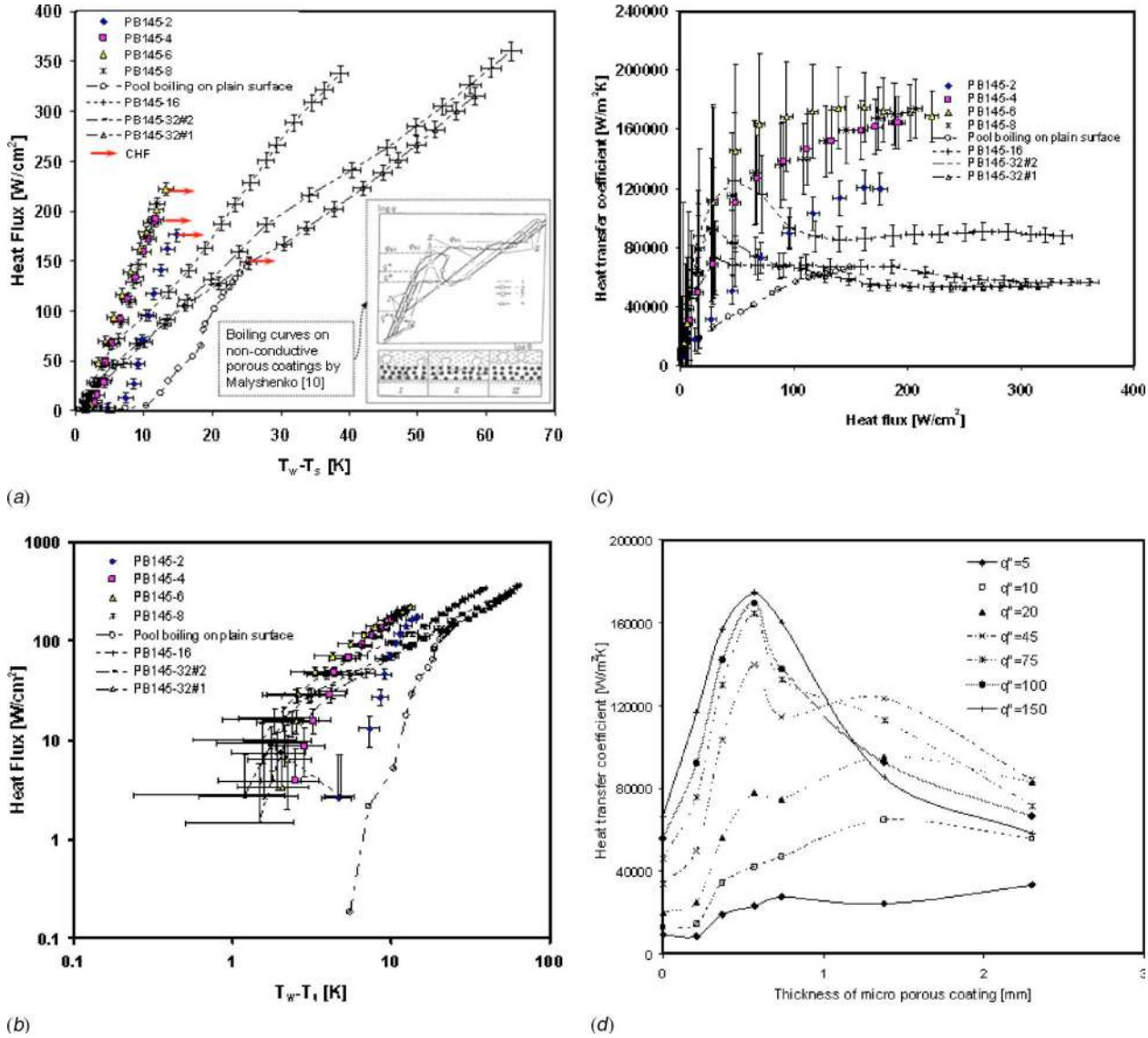

Fig. 5 (*a*) **Relationship between the heat flux and wall superheat based on the heater area as a function of thickness,** (*b*) **logarithmic relationship between the heat flux based on the heater area and wall superheat as a function of thickness,** (*c*) **relationship between the heat transfer coefficient and heat flux curve, based on the heater area as a function of thickness, and** (*d*) **relationship between boiling heat transfer performance and porous coating thickness**

this experimental study. As indicated in Figs. 5(*a*) and 5(*b*) the boiling curves of PB145-16 and PB145-32 are initially close to these test articles (i.e., PB145-4 through B145-8); however, after the heat flux exceeds a certain value, the two groups of curves begin to separate into two fairly distinct trends. This significant high wall superheat is believed to be caused by the formation of a very low conductive vapor film near the heated wall inside the porous coatings.

Assuming the vapor escapes from the top surface, the average vapor film thickness can be estimated from the test data of PB145-16 and PB145-32 using the known heat flux, thermal conductivity of vapor, and the extra temperature drop, which is the temperature difference between thin and thick wick groups at the same heat flux. The average film thicknesses for PB145-16 and PB145-32 are shown as a function of the heat flux in Fig. 6. For comparison, the thicknesses of these two porous coatings are also presented. As illustrated, the average thickness of the vapor film initially increases with increases in the heat flux, then remains relatively constant at a thickness approximately equal to, or slightly greater than, the thickness of the porous coating, which

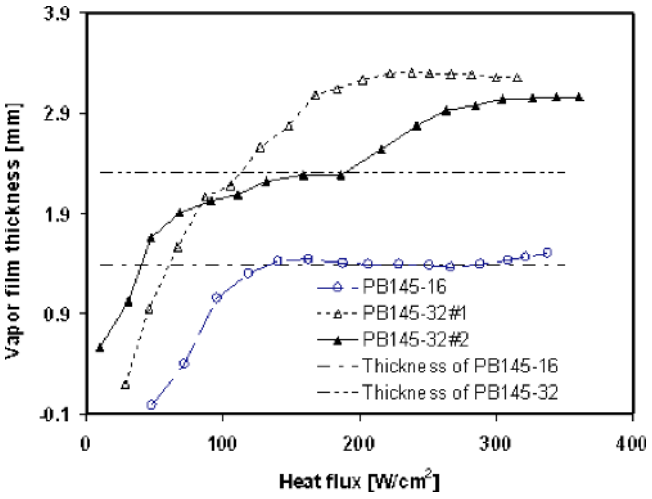

Fig. 6 Vapor film thickness as a function of heat flux at the heated wall

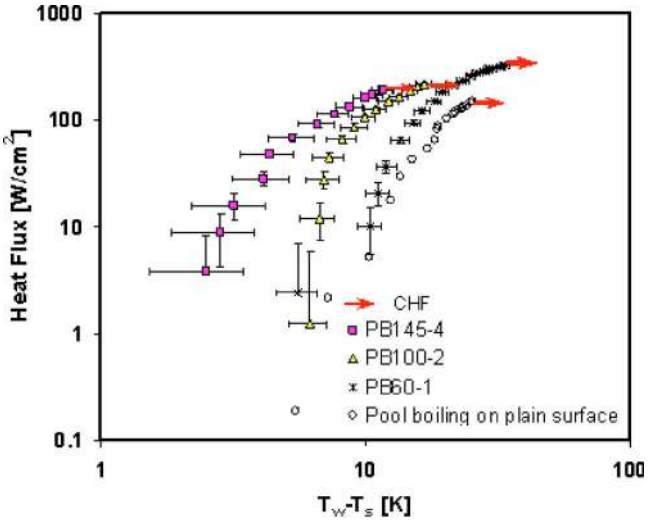

(*a*)

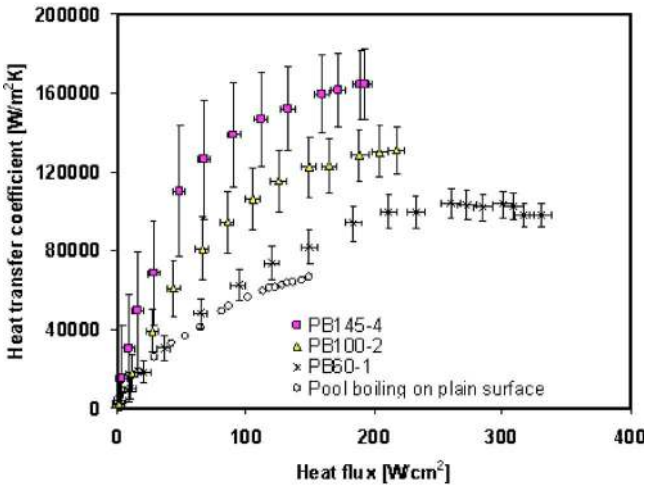

(*b*)

Fig. 7 (*a*) Logarithmic relationship between the heat flux based on the heater area and the wall superheat as a function of mesh size and (*b*) relationship between the heat transfer coefficient and heat flux based on the heater area as a function of mesh size

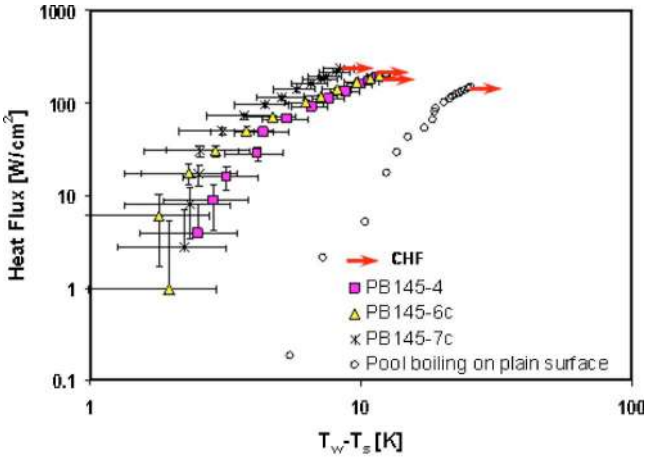

(*a*)

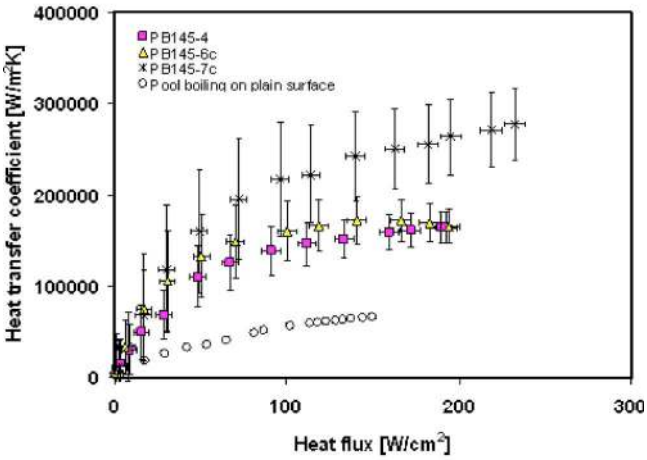

(*b*)

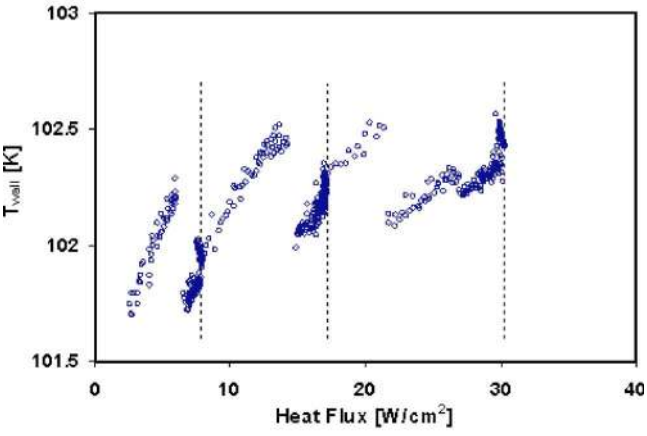

(*c*)

Fig. 8 (*a*) Logarithmic relationship between the heat flux based on the heater area and wall superheat as a function of volumetric porosity, (*b*) relationship between the heat transfer coefficient and heat flux curve based on the heater area as a function of mesh size, and (*c*) multiple boiling incipience phenomenon inside a porous media with low volumetric porosity

surprisingly does not trigger a sharp growth in the wall temperature, in other words, drying out. On the contrary, from Fig. 5(*c*) the boiling performance actually stops decreasing and remains relatively constant over a large range of heat fluxes. This phenomenon is hard to explain physically, until it is recognized that one of the assumptions, i.e., that the vapor is all vented through the top surface, may not be correct. The majority of the vapor actually escapes from the unsealed sides of thick porous coatings in most cases, which was consistent with what Moss and Kelly [13] concluded in their neutron radiography visualization and numerical modeling.

The vapor ventilation modes indicate two types of two-phase flow patterns: (i) liquid-vapor countercurrent flow, where the vapor escapes upward and the liquid flow is in the opposite direction driven by the gravity with partial assistance of capillary pressure, and (ii) liquid-vapor separating flow, where the major vapor vents through the vapor channel formed near the heater wall to the unsealed sides and the liquid enters the porous coatings from the top. The significant differences between these two flow patterns result from the vapor ventilation modes, which are mainly governed by the vapor flow resistance and the input heat flux. A theoretical analysis of the vapor flow resistance is given below to identify these parameters that govern the two-phase flow patterns.

The internal flow pressure drop is generally defined as in Eq. (4), with three assumptions: (i) vapors are generated inside porous

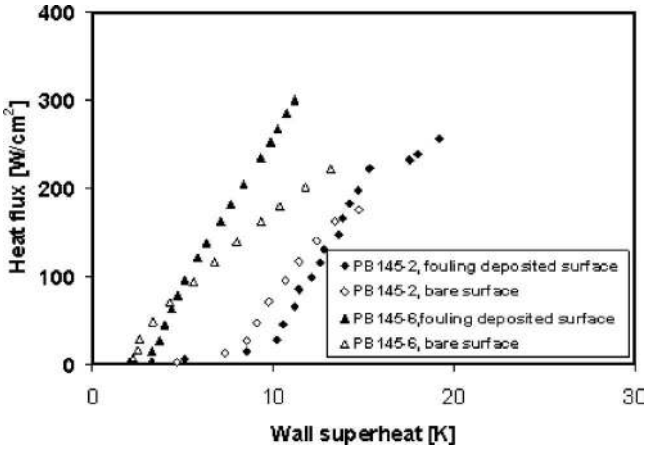

Fig. 9 Effects of surface conditions on boiling performance and characteristics for pool boiling in porous coated surfaces

media, (ii) vapor density is constant, and (iii) $f_{2\phi}$ increases with the void fraction, which also increases with input heat flux, in this case, and is generally larger than $f_{1\phi}$ at the same Re number. The vapor flow pressure equations for two phase and single phase, shown in Eq. (5), would present a theoretical analysis and be of help to explain the vapor ventilation modes.

Assuming the vapor flow resistance reaches the critical point, at which the vapor flow resistance through saturated porous media ($\Delta P_{2\phi}$) is equal to the vapor flow resistance ($\Delta P_{1\phi}$) through dry porous media, this balance can be described in Eq. (5)

$$\Delta P = \frac{1}{2} f \rho V^2 \frac{L}{D} = \frac{1}{2} f \frac{G^2}{\rho A_c^2} \frac{L}{D} \tag{4}$$

$$\Delta P_{2\phi} = \frac{f_{2\phi}(\mathrm{Re}) G_{v,2\phi}^2}{2\rho_v W_{\mathrm{heater}}^4} \frac{(t - t_{v,\mathrm{film}})}{W_{\mathrm{heater}}} = \Delta P_{1\phi}$$
$$= \frac{f_{1\phi}(\mathrm{Re}) G_{v,1\phi}^2}{2\rho_v (W_{\mathrm{heater}} t_{v,\mathrm{film}})^2} \frac{W_{\mathrm{heater}}}{\frac{4[W_{\mathrm{heater}} t_{v,\mathrm{film}}]}{2[W_{\mathrm{heater}} + t_{v,\mathrm{film}}]}} \tag{5}$$

$$G_v = \frac{q'' A_{\mathrm{heater}}}{h_{fg}} \tag{6}$$

$$\mathrm{Re}(q'') = \frac{G_v D_h}{\mu} = \frac{q'' A_{\mathrm{hetar}} D_h}{\mu h_{fg}} \tag{7}$$

where $f_{2\phi}$ and $f_{1\phi}$ are the friction factors of two-phase flow and single phase flow through wick structure, respectively; t is the wick thickness; W_{heater} is the heater characteristic size; and $G_{v,2\varphi}$ and $G_{v,1\varphi}$ are the average vapor mass flow rate through the liquid saturated (2φ) and dry porous media (1φ), respectively. They are defined in Eq. (6) and are equal. The Reynolds number is a function of input heat flux. Simplifying Eq. (5), the minimum stable vapor film thickness can be described as indicated in

$$\left(\frac{t_{v,\mathrm{film}}}{t}\right)^4 - \left(\frac{t_{v,\mathrm{film}}}{t}\right)^3 + \frac{f_{1\phi}(q'')}{2 f_{2\phi}(q'')} \left(\frac{W_{\mathrm{heatar}}}{t}\right)^3 \frac{t_{v,\mathrm{film}}}{t}$$
$$+ \frac{f_{1\phi}(q'')}{2 f_{2\phi}(q'')} \left(\frac{W_{\mathrm{heater}}}{t}\right)^4 = 0 \tag{8}$$

From this expression it is clear that the vapor film thickness is a function of $f_{2\phi}/f_{1\phi}, W_{\mathrm{heater}}/t$, and q''.

In the vapor ventilation scenario, there are two cases:

I. Vapor primarily escapes at two conditions as follows:

- When the input heat flux is small, and the $t_{v,\mathrm{film}}$ is very small; at the same time, the void fraction is also small;

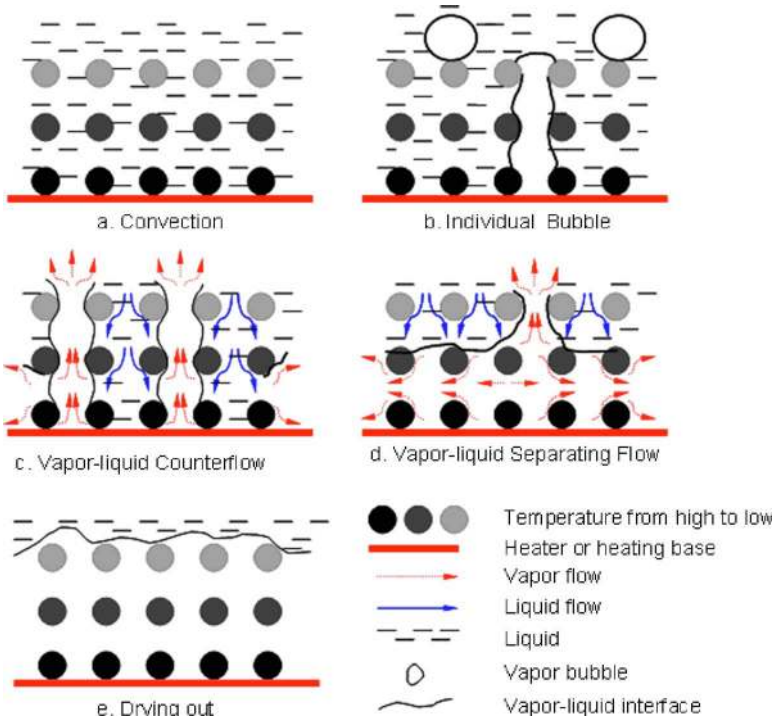

Fig. 10 Boiling and flow regimes in microconductive porous coated surfaces

thus, $f_{2\phi}$ and $f_{1\phi}$ do not vary much. From Eq. (5), $\Delta P_{2\phi}$ would be less than $\Delta P_{1\phi}$, and hence, the vapor would escape upward.
- Or the W_{heater} is much larger than the wick thickness t, which would make the vapor flow path in a single-phase channel much longer than through the liquid saturated porous media. The critical ratio of W_{heater}/t is primarily determined by the $f_{2\phi}/f_{1\phi}$.

II. Vapor primarily escapes from the unsealed sides when the W_{heater}/t is less than the critical ratio and the porous coating thickness t is larger than the minimum vapor film thickness (otherwise the surface dries out directly).

3.1.2 Heat Transfer Features. For a given heater size, there is a critical thickness t_{crit} which is equal to the minimum vapor film thickness. When the porous coating is thinner than the critical thickness t_{crit}, the boiling curve presents characteristics similar to those observed for smooth plain surfaces. Alternatively, when the porous coating is thicker than the critical thickness, the boiling curve demonstrates significantly different behaviors than those observed for smooth plain surfaces. In this latter situation, there does not appear to exist a boiling mode between nucleate boiling and film boiling, i.e., no transition boiling region, which is the case for boiling on plain surfaces. Malyshenko [10] referred to this region as "II nucleate boiling," or bubble interconnected nucleate boiling and presented similar boiling curves, as shown inside Fig. 5(*a*), based on a series of experiments on nonconductive porous coated surfaces. The observations in the current investigation are consistent with those observed by Malyshenko [10], but provided considerably more insight as to the causes and ramifications of the observed phenomena. The principal characteristics observed in this boiling region with vapor ventilation from unsealed sides can be summarized as follows:

- The heat flux does not decrease with wall superheat, but rather increases linearly with wall superheat.
- There does not exist a minimum heat flux, as in pool boiling from a plain surface during the transition from nucleate boiling to film boiling.
- The onset of film boiling is significantly delayed.
- When the vapor-liquid separating flow is formed, the CHF can be dramatically enhanced.
- The definition of the CHF for plain or thin porous coated surfaces does not appear to apply to these relatively thick porous coated surfaces.

3.2 Effect of Thickness of Microporous Coated Surfaces. In this set of experiments, the volumetric porosity and mesh size of the capillary wick were held constant, while the coating thickness was varied from 0.21 mm to 2.30 mm, to evaluate the effect of this variation on the boiling characteristics and performance. The heat flux q'' is shown as a function of the wall superheat, $T_w - T_s$, in Fig. 5(*a*), and the logarithmic relationship between these two parameters is presented in Fig. 5(*b*). The heat transfer coefficient is shown as a function of the heat flux at steady state in Fig. 5(*c*). For comparison, the boiling curve on a plain surface is also shown in Figs. 5(*a*)–5(*c*). The relationship between the boiling performance, heat flux, and thickness of the porous coatings are all illustrated in Fig. 5(*d*).

3.2.1 Effects of Thickness of Microporous Coated Surfaces on Boiling Performance. For a given heater size, previous analysis indicates that the boiling performance for conductive porous coatings is strongly dependant on the thickness. The heat transfer coefficient curve for each sample presents somewhat different characteristics. For PB145-2, the thinnest coating in this investigation, the heat transfer coefficient curve shows small improvements in the performance at low heat fluxes and significant improvements at higher heat fluxes (>28 W/cm^2) when compared to the results obtained for a smooth, plain surface. This improvement, however, is much smaller than that observed for samples PB145-4, 6, and 8. The reason for this difference is due to the combination of the reduction in the wetting area and, hence, the nucleate site density, as well as the extent of the interaction between the active nucleate sites induced by the porous coating. For samples PB145-4, 6, and 8, the performance is enhanced three to four times that of the plain surface over the entire heat flux range. This improvement is believed to be due to a combination of enhancements resulting from increases in the wetting surface area or the number of nucleation sites, the intensification of bubble interactions, and, more importantly, the introduction of the effects of the capillary and thin-film evaporation [8–12,15,16,19,20]. Furthermore, the performance of samples PB145-4, 6, and 8 do not show significant differences, which indicates that the wetting area does not always impact the boiling performance and that the principal evaporation and nucleate boiling may occur solely inside the porous coatings in the vicinity of the heating wall when the effective thermal conductivity is not sufficiently high, which was strongly supported by the phenomena observed from the sample PB145-7c in Sec. 3.4. On the sample PB145-7c, which has the highest thermal conductivity in this experimental investigation, the evaporation position is found to move upward with the heat flux increase on the highly conductive porous coatings. This observed effect of the wetting area on boiling performance also implies that heat is conducted through the solid structure of the porous media to the saturated working fluid. Thus, the boiling performance can be enhanced by augmenting the effective thermal conductivity of porous coatings. This principle was illustrated by Polezhaev and Kovalev [17] in their numerical simulations.

Because of the existence of a thin vapor film, the boiling curves for PB145-16 and PB145-32 indicate significant differences when compared to the thinner samples. As shown in Fig. 5(*a*), the performance of PB145-16 is superior to that of PB145-32 over the entire range of heat fluxes evaluated. From these two test articles, the heat transfer coefficient on both of them increased with increasing heat flux and decreased after the heat fluxes exceed a specific value, ultimately converging to a constant value. For PB145-16, the inflection point was ~ 48 W/cm^2, and for PB145-32, the value was ~ 30 W/cm^2. This inflection point seems to decrease with an increase in coating thickness. Malyshenko [10] hypothesized that this was due to the heating surface being blocked by a thin stable vapor film, established within the body of the porous coatings. Nakayama et al. [15] found that porous structures with heat fluxes of >15 W/cm^2, the boiling curves of the porous structures converged towards the boiling curve of a plain surface. This decrease in performance was attributed to the "dried-up" mode of boiling. In addition, it was hypothesized by Nakayama et al. [15] that the structure would revert toward plain surface behavior once the tunnel space was filled with vapor.

Combining the observations of the current investigation with those of other researchers as described in the Introduction, it is evident that the formation of a vapor film is responsible for this significant change in the boiling performance. As indicated in the previous analysis, the specific causes that led to the formation of the vapor film, may be due to the high flow resistance of the vapor, as it attempts to escape through the saturated porous media [10,13,14]. It is important to note that the boiling heat transfer is not terminated by the presence of the vapor film; on the contrary, stable boiling accompanied by high wall superheat has been observed in both the current investigation and in those of other researchers [10–12,15] for both conductive and nonconductive thick porous coatings.

The effect of variations in the heat flux on the boiling heat transfer coefficient is illustrated in Fig. 5(*d*) as a function of the porous coating thickness, in order to demonstrate the relationship between the boiling performance, the microporous surface thickness, and the heat flux. As shown, the boiling heat transfer coefficient is strongly dependent on the wick thickness and the heat flux when the heater size is given. When the heat flux is lower

than $\sim 20\ W/cm^2$, the boiling performance was found to increase with increases in the porous coating thickness. For highly conductive porous coatings in the present investigation, the solid portion of the porous structure effectively conducts the heat for low to moderate input power levels and reduces the effective heat flux. However, at higher input power levels, the heat transfer is greater than what can be readily transferred. For example, when the heat flux is $>20\ W/cm^2$, the boiling performance increases with increasing thickness for coating thicknesses of <0.57 mm and then decreases with additional increases in the thickness beyond that value. The observed differences between the current investigation and the results of Malyshenko [10] are believed to be due to the very different thermal conductivities of the porous coating materials, i.e., highly conductive porous media in the present study and relatively nonconductive porous media in the investigation of Malyshenko [10].

3.2.2 Boiling Incipience Superheat. Figure 5(*b*) clearly illustrates that nucleate incipience superheat for most samples is dramatically reduced through the application of a porous coating. This is consistent with the findings of other researchers that have experimented with enhanced structures and surfaces [5–20]. Virtually all of these investigations have indicated that "rough surfaces" are an effective mechanism for reducing the boiling incipience superheat. This is due to the combination of artificial cavities with large pore sizes within the porous coating [16] and the thermocapillary convection that occurs in the liquid film on the walls of the coating materials, all of which result in a reduction in the boiling incipience superheat in conductive porous coated surfaces [10–12]. As illustrated in Fig. 5(*b*), the boiling incipience superheat for relatively thin, i.e., for test article PB145-2, is not reduced significantly, even though the geometric characteristics of the heated wall are identical to other thicker porous layers. These observations indicate that thickness is one of the factors that affect the boiling incipience superheat on surfaces coated with a conductive porous media.

3.3 Effects of Mesh Size of Microporous Surfaces on Performance and Characteristics. Another series of experiments was conducted in which the thickness and volumetric porosity of the porous coatings were both maintained at approximately the same value while the mesh size was varied from 2362 m^{-1} (60 $in.^{-1}$) to 5709 m^{-1} (145 $in.^{-1}$) and with the variation of the wire diameters. All these geometric parameters are listed in Table 1. This allowed the evaluation of the effect of pore size on the boiling performance and characteristics. Test data from this series of tests are presented in Figs. 7(*a*) and 7(*b*). The boiling curve for a plain surface is added to these Figs. 7(*a*) and 7(*b*) for comparison.

As illustrated in Fig. 7(*a*), the boiling incipience superheat for this set of experiments shows a fairly large variation when the mesh size varies. The boiling incipience superheat of test article PB145-4 is significantly smaller than those of PB100-2 and PB60-1, which are almost identical with that obtained for a plain surface. For the sintered copper mesh used in the present work, the pore size in the horizontal direction increases as the mesh size decreases, which implies that only the pore size in a specific range will affect the boiling incipience superheat. When the pore size is too small or too large, the boiling incipience superheat is determined by the surface condition of the heated wall or wire surfaces, rather than the pore size of the porous coating.

Figure 7(*b*) illustrates the effects of the mesh size on the boiling performance. As indicated, the performance decreases with increasing mesh size. This phenomenon is believed to be due to the decrease in the wetting area and/or number of nucleation sites available as the mesh size increases. In a previous investigation, Li and Peterson [21] showed that the effective thermal conductivity of porous surfaces fabricated from mesh screens increases with the product of the mesh number and wire diameter. This factor may also contribute to this performance decrease since the effective thermal conductivity would decrease with increasing mesh size [17]. The boiling performance of test article PB60-1, which was fabricated from a relatively coarse mesh, is very close to that of a plain surface when the heat flux is $<50\ W/cm^2$. Because of the beginning of the film evaporation on the upper part of the coatings, the performance is only slightly better than that of a plain surface when the heat flux exceeds $50\ W/cm^2$. This observation indicates that boiling initially occurs on the heated wall and then progresses through the solid structure for the porous coating once the superheat reaches a level that is directly related to the heat flux.

3.4 Effects of Volumetric Porosity of Microporous Coated Surfaces on Boiling Performance and Characteristics. The effects of volumetric porosity on boiling performance and characteristics were also examined while holding the thickness and mesh size constant. The volumetric porosity investigated here ranged from 0.409 to 0.693 and was achieved by reducing the distance between the layers in the vertical direction (i.e., normal to the heater surface direction), while the pore size does not change in the horizontal direction. The experimental test data are illustrated in Figs. 8(*a*)–8(*c*). As was the case for the previous results, the boiling curve for a plain surface is also illustrated for comparison.

As shown, the boiling incipience superheats for test articles PB145-4, PB145-6c, and PB145-7c are approximately identical and much smaller than those of a plain surface. The pore size in the horizontal direction and the thicknesses of the three samples was held constant, with only the pore size in the vertical direction varied to change the volumetric porosity. The results indicate that the boiling incipience superheat is nearly independent of pore size in the vertical direction, and as a result, the pore size in the horizontal direction and the thickness of the porous coating seems to show a significantly greater effect in determining boiling incipience superheat for a given working fluid and pressure.

A significant enhancement in the boiling performance is demonstrated in Fig. 8(*b*) and increases with a decrease in the volumetric porosity. It is interesting to note that the effective thermal conductivity of the porous coating changes with variations in the volumetric porosity. Generally, for a given porous structure, the effective thermal conductivity of the porous media would increase with decreases in the volumetric porosity. This increase in the effective thermal conductivity contributes to the boiling performance increase for test article PB145-7c. An additional phenomenon, shown in Fig. 8(*c*), can be observed for test article PB145-7c, which has the lowest volumetric porosity and, hence, the highest effective thermal conductivity of all the test articles. As illustrated in Fig. 8(*c*), for test article PB145-7c the wall temperature increases initially with the heat flux and then drops several degrees due to the higher heat transfer mode. This same phenomenon was observed in three separate tests conducted to ensure the results were repeatable and indicates that multiple boiling modes, i.e., the nucleate boiling position spread from the bottom to the top of the porous coating, could occur simultaneously in these types of porous coatings when the effective thermal conductivity is high enough, which is what was observed previously for finned surfaces [22] and predicted in the numerical simulation by Polezhaev and Kovalev [17]. Initially, nucleate boiling occurs near the heated wall and then moves through the porous coating as the heat flux is increased. This multiple boiling incipience phenomenon results in a much higher boiling performance for test article PB145-7c than for PB145-6c and provides strong evidence from which to support the conclusions presented in Sec. 3.2.1, i.e., the heat is conducted through the skeleton of the porous media and is then dissipated to the liquid through the surface of the porous coating.

3.5 Effects of Microporous Coated Surfaces on Wall Superheat. As shown in Figs. 5(*b*), 7(*a*), and 8(*a*), with the exception of test articles PB145-16, PB145-32, and PB60-1, the wall superheat at the CHF, $\sim 12^\circ C$, is much less than that obtained for

a plain surface at 25 °C. This implies that the boiling heat transfer in porous coatings is more stable in terms of the wall temperature than for plain surfaces and as a result, provides a superior temperature control method for thermal management.

3.6 Effects of the Surface Condition of the Wires. The effects of surface conditions on boiling performance were also investigated as part of this study. To accomplish this, the surface of the porous coatings were initially saturated with water and heated to 300–400 °C to generate a thin oxide film on the individual wires in the mesh. These surfaces were then carefully cleaned using a solution of DuracleanTM 1075 to form a thin porous structure on the surfaces of the wires prior to the tests. This thin porous structure was similar to the type of surface often found on fouled heat exchanger tubes. Figure 9 presents and compares the results of tests conducted on both oxide-coated and uncoated samples. As illustrated, from a boiling perspective the bare surfaces performed better than those with the oxide layer when the heat flux was low for test article PB145-2 and low to moderate for test article PB145-6; however, as the heat flux increased to a level of 75 W/cm^2 and 175 W/cm^2 for PB145-2 and PB145-6, respectively, the performance of the oxide-coated surfaces quickly exceeded that of the bare wires. This phenomenon can be attributed to the existence of the extra thermal resistance resulting from the deposited layer, which approximates the fouling of the surfaces. When the heat flux is relatively small, the superheat on bare surfaces is higher than on the oxide-coated surface, which means there are more active nucleation sites on the bare surface than on the oxide layers, which can easily trigger nucleate boiling. These observations are consistent with the findings of Fukada et al. [23].

4 Boiling Regimes and Two-Phase Flow Pattern on Conductive Porous Coated Surfaces

Based on a review of the literature, the experimental investigations form both the current investigation and the theoretical analysis, a new set of boiling regimes have been developed as shown in Fig. 10. Summarily, when the ratio W_{heater}/t is larger than a critical ratio, which is mainly governed by the $f_{2\phi}/f_{1\phi}$ ratio, the heat transfer typically consists of four regimes: (a) convection, (b) boiling with individual bubble, (c) vapor-liquid counterflow and boiling, and (d) drying out. While the ratio W_{heater}/t is relatively small and, hence, vapor may vent from unsealed sides at high heat flux, there is one more heat transfer regime remaining after the vapor-liquid counterflow, i.e., the so-called two-phase separating flow and boiling (regime e).

As shown, the pool boiling on highly conductive porous coated surfaces starts from a regime best described as convection (i.e., regime a). With an increase in the heat flux, many individual bubbles are generated in the sharp corner regions between the individual wires, and between the heated wall and the wire surfaces, all of which result in the onset of boiling. Bubbles rising through the porous coating strengthen the convection in the upper part of the porous coated surfaces, regime b, which essentially serves as a transition regime for boiling on conductive porous coated surfaces. Single bubbles then coalesce to form a bubble stem, or slug, with further increases in the heat flux, in regime c. In this process, the bubble population above the porous surface is fairly stable and is further supported by the nearly linear relationship between the heat flux and the wall superheat [24]. Kim et al. [25] attributed this to the constant nucleation site density in the porous coated surfaces. Another important feature in this regime is that a strong liquid vapor counterflow pattern is established. This two-phase counterflow enhances the heat transfer, but also makes it more difficult for the liquid to reach the bottom of the porous coated surfaces.

When the CHF is reached for the relatively thin highly conductive porous coated surfaces, the vapor velocity is sufficiently high to retard or prevent this liquid resupply due to the flow resistance through the porous media and the shear stress generated by the high vapor velocities. Bubbles above the porous coated surface in violent motion, block the top surface of the porous coated surfaces, causing film boiling to occur, i.e., regime e. This begins in a manner identical to that of a smooth surface, with the difference being that the mushroom bubbles are further from the heated wall, due to the vapor jets from the porous coated surfaces. This enhances the heat transfer and CHF from the porous coated surfaces when compared to a plain surface.

For boiling on the relatively thick porous coated surfaces with small areas, open sides, and a sufficiently high heat flux, the vapor flow is quite fast, making it difficult for the vapor to escape through the thick saturated porous media. As a result, the vapor takes the path of least resistance through the thin vapor film layer near the heated wall [14,20]. The thickness of this vapor film increases with increasing heat flux and, when it reaches the same thickness as the porous coating, the CHF occurs. In regime d, boiling still occurs in the upper portion of the porous coated surface, but the majority of the heat is dissipated through evaporation at the vapor liquid interface close to the heated wall. The overall heat transfer in regime d is low because of the high thermal resistance caused by the stable vapor film between the heated wall and the liquid vapor interface.

5 Conclusions

The effects of the key geometric parameters of conductive microporous surfaces have been systematically investigated using saturated distilled water on horizontal surfaces. The test results demonstrated that the boiling characteristics and overall boiling performance are strongly dependent on the geometric parameters of the porous coatings, i.e., thickness, volumetric porosity, and mesh size, when the heater size and the pressure are held constant. More importantly, the enhanced understanding of the specific characteristics of boiling in and on conductive microporous coated surfaces is revealed and discussed.

The normal heat transport route in pool boiling from a porous coated surface was found to be the result of heat conducted to the skeleton of the porous structure and then transferred to the liquid through convection and, finally, dissipated through boiling or evaporation on the surface of the porous coatings. In addition, two types of liquid-vapor flow patterns are identified at a high heat flux, i.e., vapor liquid counterflow and liquid-vapor separating flow. A theoretical analysis indicates that the liquid-vapor flow patterns are generally governed by the ratio W_{heater}/t, $f_{2\phi}/f_{1\phi}$, and the input heat flux q''.

In general, the boiling characteristics from porous coated surfaces are generally superior to that of pool boiling on plain surfaces. The mechanisms of improvement are mainly due to the augmentation of the wetted area, the number of nucleation sites, the intensified interaction among bubbles, as well as film and capillary evaporation induced through the use of porous coatings. Porous coatings with higher thermal conductivity were found to perform better than those with lower thermal conductivities, especially at low heat fluxes.

The boiling incipience superheat can be significantly reduced through the use of porous coatings and the boiling incipience superheat can be controlled by varying either the pore size or the thickness of the porous coating. The experimental results demonstrated that boiling on thin porous coatings could occur over a larger range heat flux, i.e., from 0 to 210 W/cm^2, and at the same time, within a much narrower wall superheat, i.e., <12 °C, than for plain surfaces. This indicates that the boiling heat transfer on thin porous coatings is more stable in terms of temperature and, hence, may be more suitable for applications where precise temperature control is required.

Acknowledgment

The authors would like to acknowledge the support of the National Science Foundation under Grant No. CTS-0312848.

Nomenclature

A_c = cross area (m^2)
D = diameter (mm)
D_h = hydraulic diameter (mm)
F = friction factor
G = mass flow rate (kg/s)
H = heat transfer coefficient ($W/m^2 K$)
h_{fg} = latent heat (kJ/kg)
K = thermal conductivity (W/mK)
ΔP = pressure drop (Pa)
q'' = heat flux (W/cm^2)
Re = Reynolds number
L = length (mm)
t = distance or thickness (mm)
T = temperature (K)
TC = thermocouple
V = speed (m/s)
W = width (mm)

Greek Symbols

σ = surface tension (N/m)
ρ = density (kg/m^3)
ε = volumetric porosity
1ϕ = single-phase
2ϕ = two-phase

Subscripts

crit = critical parameter
gap = gap between the vapor zones or columns
heater = dimensions of heater
l = liquid phase
v = vapor phase
v, film = dimensions of vapor film
w = wall
sat = saturation condition
eff = effective parameter
Cu = copper
hole = holes in the heater to hold the thermocouples
STC1 = top surface of copper block to TC1

References

[1] Jakob, M., 1949, *Heat Transfer*, Wiley, New York, pp. 636–638.
[2] Milton, R. M., 1968, "Heat Exchange System," U.S. Patent No. 3384154.
[3] Milton, R. M., 1970, "Heat Exchange System," U.S. Patent No. 3523577.
[4] Milton, R. M., 1971, "Heat Exchange System with Porous Boiling Layer," U.S. Patent No. 3587730.
[5] You, S. M., Simon, T. W., and Bar-Cohen, A., 1992, "A Technique for Enhancing Boiling Heat Transfer With Application to Cooling of Electronic Equipment," IEEE Trans. Compon., Hybrids, Manuf. Technol., **15**(5), pp. 823–831.
[6] O'Connor, J. P., and You, S. M., 1995, "A Painting Technique to Enhance Pool Boiling Heat Transfer in Saturated FC-72," ASME J. Heat Transfer, **117**(2), pp. 387–393.
[7] O'Connor, J. P., You, S. M., and Price, D. C., 1995, "A Dielectric Surface Coating Technique to Enhance Boiling Heat Transfer from High Power Microelectronics," IEEE Trans. Compon., Packag. Manuf. Technol., Part A, **18**(3), pp. 656–663.
[8] Chang, J. Y., and You, S. M., 1997, "Boiling Heat Transfer Phenomena From Micro Porous and Porous Surfaces in Saturated FC-72," Int. J. Heat Mass Transfer, **40**(18), pp. 4437–4447.
[9] Liter, S. G., and Kaviany, M., 2001, "Pool-Boiling CHF Enhancement by Modulated Porous-Layer Coating: Theory and Experiment," Int. J. Heat Mass Transfer, **44**, pp. 4287–4311.
[10] Malyshenko, S. P., 1991, "Characteristics of Heat Transfer With Boiling on Surfaces With Porous Coatings," Therm. Eng., **38**(2), pp. 81–88.
[11] Borzenko, V. I., and Malyshenko, S. P. "Experimental Research of Heat Transfer Enhancement and Thermal Stability at Pool Boiling in Porous Surfaces," Heat Transfer Science and Technology, Beijing, pp. 492–502.
[12] Borzenko, V. I., and Malyshenko, S. P., 2001, "Mechanisms of Phase Exchange Under Conditions of Boiling on Surfaces With Porous Coating," High Temp., **39**(5), pp. 769–776.
[13] Moss, R. A., and Kelly, A. J., 1970, "Neutron Radiographic Study of Limiting Plannar Heat Pipe Performance," Int. J. Heat Mass Transfer, **13**, pp. 491–502.
[14] Cornwell, K., Nair, B. G., and Patten, T. D., 1976, "Observation of Boiling in Porous Media," Int. J. Heat Mass Transfer, **19**, pp. 236–238.
[15] Nakayama, W., Daikoku, T., Kuwahara, H., and Nakajima, T., 1980, "Dynamic Model of Enhanced Boiling Heat Transfer in Porous Surfaces—Part I: Experimental Investigation," ASME J. Heat Transfer, **102**, pp. 445–450.
[16] Bergles, A. E., and Chyu, M. C., 1982, "Characteristics of Nucleate Pool Boiling From Porous Metallic Coatings," ASME J. Heat Transfer, **104**, pp. 279–285.
[17] Polezhaev, Y. V., and Kovalev, S. A., 1990, "Modeling Heat Transfer With Boiling in Porous Structures," Therm. Eng., **37**(12), pp. 617–620.
[18] Vemuri, S., and Kim, K. J., 2005, "Pool Boiling of Saturated FC-72 on Nano-Porous Surface," Int. Commun. Heat Mass Transfer, **32**, pp. 27–31.
[19] Li, C., Peterson, G. P., and Wang, Y., 2006, "Evaporation/Boiling on Thin Capillary Wick (I)—Wick Thickness Effects," ASME J. Heat Transfer, **128**. pp. 1312–1319.
[20] Li, C., and Peterson, G. P., 2006, "Evaporation/Boiling on Thin Capillary Wick (I)—Effects of Volumetric Porosity and Mesh Size," ASME J. Heat Transfer, **128**. pp. 1320–1328.
[21] Li, C., and Peterson, G. P., 2006, "The Effective Thermal Conductivity of Wire Mesh," Int. J. Heat Mass Transfer, **49**, pp. 4095–4105.
[22] Haley, K. W., and Westwater, J. W., 1966, "Boiling Heat Transfer from a Single Fin," *Proceedings of the ASME/AIChE National Heat Transfer*, Chicago, IL, Vol. 3, pp. 245–253.
[23] Fukada, Y., Haze, I., and Osakabe, M., 2004, "The Effects of Fouling on Nucleate Pool Boiling of Small Wires," Heat Transfer Asian Res., **33**(5), pp. 316–329.
[24] Bejan, A., and Kraus, A. D., 2003, *Heat Transfer Hand Book*, Wiley, New York, pp. 704–705.
[25] Kim, J. H., Rainey, K. N., You, S. M., and Pak, J. Y., 2002, "Mechanism of Nucleate Boiling Heat Transfer Enhancement From Microporous Surface in Saturated FC-72," ASME J. Heat Transfer, **124**(3), pp. 500–506.